Improved detection of volcanic sulphur dioxide using infrared imaging radiometers

Forecasting Research Technical
Report No: 577

May 2013
Michael Cooke

Contents

Abstract **2**

1. Introduction **2**

1.1 The need to improve the current sulphur dioxide product..... 4

2. Methodology: Sulphur dioxide detection **6**

3. Detection Results **7**

4. Quantitative estimate of column loading **10**

5. Limitations of sulphur dioxide detection from infrared imagers **16**

6. Conclusions **18**

Bibliography **19**

Abstract

A method for the detection of sulphur dioxide using infrared imaging radiometers is proposed. Measured radiances and numerical weather predication (NWP) model data are used to retrieve a layer emissivity which is more sensitive to the layer physics than are methods based solely on measured brightness temperatures. Improved sensitivity to sulphur dioxide was shown relative to a method using brightness temperature data alone. The estimated sulphur dioxide column loading values were compared qualitatively and quantitatively with retrieved values from a hyperspectral sounder (AIRS). The qualitative evaluation showed good spatial agreement. Quantitative sulphur dioxide estimates were generated from MODIS and SEVIRI data using a method of best fit between layer emissivity and AIRS derived sulphur dioxide column loading. A linear fit provided an estimate of the absorption coefficient for sulphur dioxide for a given imager channel. This allowed an estimate of the sulphur dioxide column loading to be generated from the imagers. The estimated column loadings from MODIS and SEVIRI were in good agreement with AIRS derived column loadings.

1. Introduction

The London Volcanic Ash Advisory Centre (VAAC), hosted by the Met Office (UK), has the responsibility to issue volcanic ash advisories for the Icelandic region to provide guidance to the Civil Aviation Authority (CAA). A better understanding of the plumes generated during a volcanic eruption will allow for improved advice. The ability to detect and track sulphur dioxide rich volcanic plumes is complementary to volcanic ash tracking and helps the London VAAC improve its advice to the CAA.

Sulphur dioxide is a colourless gas that can cause eye irritation and breathing difficulties. It is, typically, the third most abundant gas emitted from a volcano (after water vapour and carbon dioxide) and the annual global volcanic emissions correspond to 10-15 % of the anthropogenic emissions (Halmer et al., 2002). The background atmosphere contains very little sulphur dioxide because its emissions are typically in the boundary layer where dry and wet deposition readily remove it (lifetime ~ 1 day due to dry deposition in the boundary layer and ~ 1 week via reaction with the hydroxyl radical in the free troposphere).

Visible and infrared imaging radiometers are used to track volcanic plumes that contain both ash and sulphur dioxide. The spinning enhanced visible and infrared imager (SEVIRI) is flown on Meteosat Second Generation (MSG) which is a geostationary satellite positioned above the equator at 0° longitude. SEVIRI provides high temporal (every 15 minutes) and spatial resolution (3x3 km at nadir) which makes it an important tool for nowcasting applications. The moderate resolution imaging spectroradiometer (MODIS) is flown on Terra and Aqua satellites which are polar orbiting platforms. The two MODIS instruments together provide approximately 4 images of the London VAAC area per day with a spatial resolution of 1x1 km for nadir views.

Sulphur dioxide has three absorption bands in the mid-infrared. A strong absorption band between 7.2 µm and 7.5 µm from the ν_3 asymmetric stretch, a band between 7.8 µm and 8.6 µm from the ν_1 symmetric stretch and the weak combination band (ν_1 and ν_3) between 3.9 µm and 4.5 µm. These bands correspond, conveniently, with channels 4, 6 and 7 for SEVIRI and bands 22, 28 and 29 for MODIS, see table 1.

The weak absorption at 4.0 µm is difficult to use because this is a region where there are both solar and thermal components to the measured radiances. Several techniques have been used for sulphur dioxide detection in the 7.3 µm and 8.7 µm regions. The window channel at 8.7 µm has a weaker sulphur dioxide absorption but has been used successfully for detection throughout the atmospheric column (Watson et. al, 2004). The strong absorption at 7.3 µm overlaps with a water vapour absorption band making this only suitable for detecting sulphur dioxide plumes which are above the majority of atmospheric water vapour (~ 3 km, Prata et al., 2003).

Table 1: The SO_2 absorption bands in the infrared part of the electromagnetic spectrum in comparison with the appropriate instrument channels on the SEVIRI and MODIS instruments.

SO_2 band (µm)	SEVIRI band (µm)	SEVIRI channel	MODIS band (µm)	MODIS channel
3.9 – 4.5	3.48 - 4.36	4	3.929-3.989	22
7.2 – 7.5	6.85 - 7.85	6	7.175-7.475	28
7.8 – 8.6	8.30 - 9.10	7	8.400-8.700	29

The aim of this study is to present a simple method which can be used to improve the detection of sulphur rich volcanic plumes by incorporating numerical weather prediction (NWP) model data into the detection process.

1.1 The need to improve the current sulphur dioxide product

During the Grimsvötn eruption in May – June 2011 a large sulphur dioxide plume with little ash was seen to be transported north of Iceland while the bulk of the volcanic ash was transported south towards the UK. This can be seen in the dust RGB image in figure 1(a) where the sulphur dioxide plume is coloured green and heading north with the ash rich plume (a bright red colour) to the south-east partially overlapped by frontal ice cloud which is a darker red colour.

Figure 1 shows an example of the current volcanic sulphur dioxide product which is based on the brightness temperature difference method employed in Prata et al. (2003) with updates given in Doutriaux-Boucher and Dubuisson (2009). In this method the SEVIRI channels at 6.2 µm and 10.8 µm are used to estimate the "expected radiance" in the 7.3 µm channel using linear interpolation and assuming no sulphur dioxide is present. The measured and expected radiances at 7.3 µm are converted to brightness temperatures. A brightness temperature difference (BTD) is evaluated, viz

$$BTD = BT^{e}(7.3\mu m) - BT(7.3\mu m) \qquad \textbf{Eq. 1}$$

$$mean(BTD) = \frac{\sum_{i=1}^{i=n} BTD}{n} \qquad \textbf{Eq. 2}$$

where BT^{e}(7.3 µm) is the expected brightness temperature at 7.3 µm, BT(7.3 µm) is the measured brightness temperature at 7.3 µm, n is the number of pixels in a given image area and mean(BTD) is the mean brightness temperature difference for a given image area. Figure 1(b) shows the operational product where the BTD threshold is 2.5 times the mean(BTD) (2.5*mean(BTD)), where mean(BTD) is generated using equation 2. This fails to detect the majority of the volcanic sulphur dioxide plume as it is transported northwards. Figure 1(c) and 1(d) show what happens when the threshold value is relaxed. The volcanic sulphur dioxide is detected but with the downside of increasing the amount of false detected pixels particularly over high clouds and land surfaces.

The aim of this study is to use a framework which is more sensitive to the layer physics and less sensitive to the surface emissivity, surface temperature, atmospheric temperature, and atmospheric water vapour. This can be achieved by combining

observed radiances and modelled radiances produced using a radiative transfer code (RTTOV, Hocking et al., 2011).

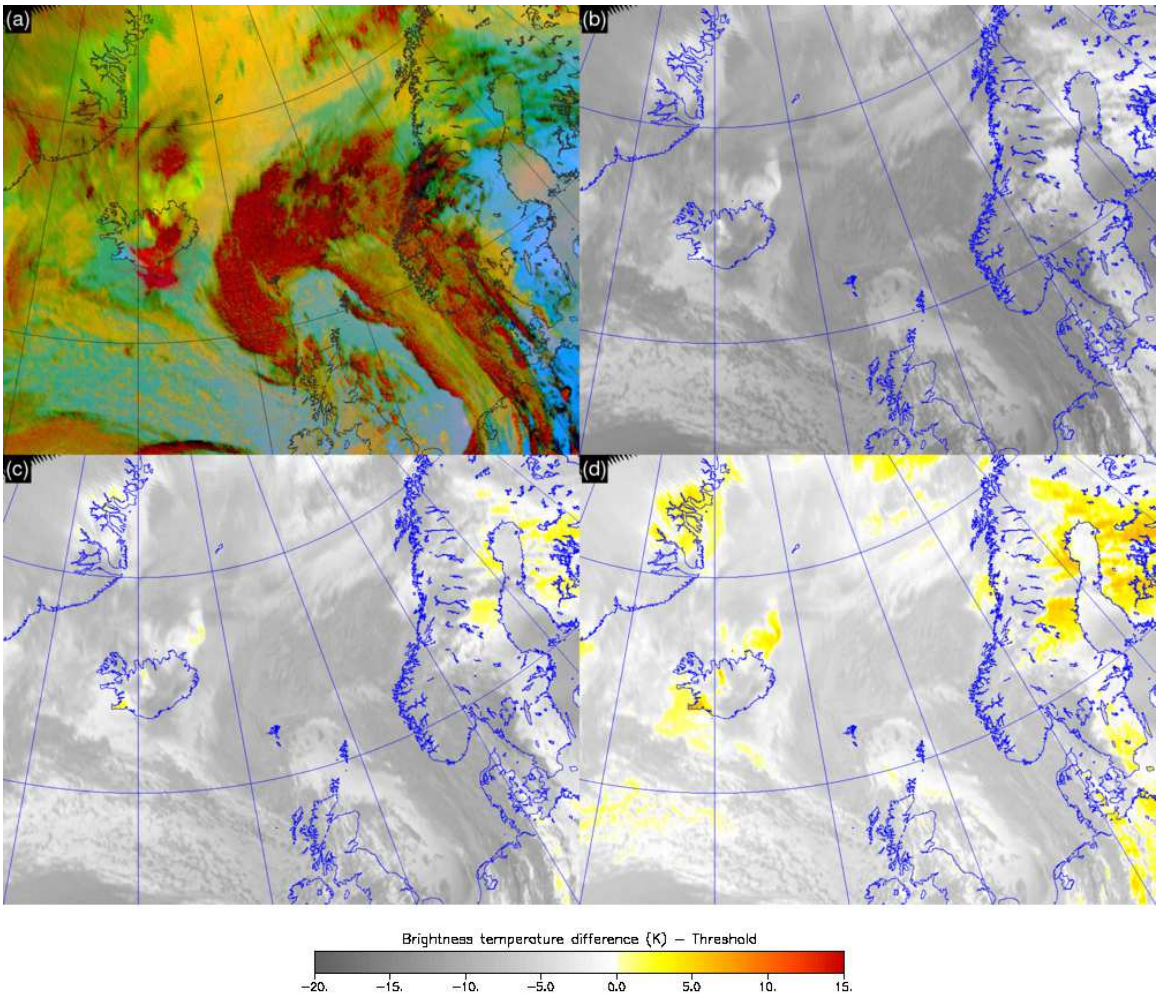

Figure 1: SEVIRI images from 22/05/2011 between 10:45 and 11:00 UTC. (a) Dust-RGB which shows the sulphur dioxide rich plume to the North of Iceland (green) with the ash rich plume to the south of Iceland (bright red) which is partially covered by frontal cloud. (b), (c) and (d) show sulphur dioxide images using the brightness temperature difference (BTD) technique described in section 1.1 with different thresholds. (b) threshold = [2.5*mean(BTD)]. (c) threshold = [2.0*mean(BTD)]. (d) threshold = [1.5*mean(BTD)]. The colour bar shows the deviation from the assigned threshold for panels (b), (c) and (d).

2. Methodology: Sulphur dioxide detection

The method employed in this paper uses the strong absorption band in the 7.3 µm water vapour channel for detection and the 8.5-8.7 µm channel for producing a quantitative estimate. The detection technique applied to SEVIRI and MODIS data uses the "effective cloudy emissivities" approach described in detail by Pavolonis (2010). This allows for surface variations to be taken into account by using information from a NWP model and is a robust alternative to brightness temperature differences (Pavolonis, 2010). Kuhn (1963) showed that in a non-scattering atmosphere with a fully cloudy field of view and negligible contribution from downwelling cloud or molecular emissions the radiative transfer equation can be written as:

$$R_{obs}(\lambda) = \varepsilon(\lambda)R_{ac} + t_{ac}(\lambda)\varepsilon(\lambda)B(\lambda, T_{eff}) + R_{clr}(\lambda)(1-\varepsilon(\lambda)) \quad \textbf{Eq. 3}$$

where R_{obs} is the observed radiance, λ is the wavelength, R_{clr} is the clear sky radiance, R_{ac} is the radiance emitted (upwards towards the satellite) by the atmosphere above the layer and t_{ac} is the transmittance above the layer. B is the Planck function and T_{eff} is the effective layer temperature. ε is the cloud emissivity. The temperature is an effective temperature because it is the effective temperature of the emitting layer, not the layer top temperature. Equation 3 can be re-arranged to be given in terms of the layer emissivity viz.

$$\varepsilon(\lambda) = \frac{R_{obs}(\lambda) - R_{clr}(\lambda)}{R_{cld}(\lambda) - R_{clr}(\lambda)} \quad \textbf{Eq. 4}$$

$$R_{cld}(\lambda) = B(\lambda, T_{eff})t_{ac}(\lambda) + R_{ac}(\lambda) \quad \textbf{Eq. 5}$$

where R_{cld} is the radiance observed at the satellite if an opaque layer was located at T_{eff}. The physical information of a layer cannot be captured using an emissivity at one wavelength; it is the variation with wavelength that contains the information. Equations 3 to 5 are used to distinguish between water, ice and sulphur dioxide layers. The theory has been derived for the radiative effects of cloud but is being used here for a layer of gas. This is justifiable because sulphur dioxide absorbs strongly at 7.3 µm in a similar manner to a water or ice cloud. The single layer tropopause assumption is used to calculate the layer emissivity for a given pixel. In this assumption the layer emissivity is calculated assuming an opaque layer (R_{cld}) at the thermodynamic tropopause given from NWP data. The tropopause approximation is used because the majority of volcanic

plumes will be in the troposphere. If there were prior knowledge of the plume height it would be possible to improve upon the assumption. The sulphur dioxide plume is detected using the variation in layer emissivity with wavelength and thus the consequences of using an incorrect plume temperature should not adversely affect the detection.

The thresholding used for the detection of a sulphur dioxide plume is:

$$\varepsilon(7.3\mu m) > \varepsilon(6.2\mu m) \quad \textbf{Eq. 6}$$
$$\varepsilon(7.3\mu m) > \varepsilon(12.0\mu m) \quad \textbf{Eq. 7}$$
$$\varepsilon(7.3\mu m) > \varepsilon(13.4\mu m) \quad \textbf{Eq. 8}$$
$$\varepsilon(7.3\mu m) > 0.2 \quad \textbf{Eq. 9}$$

The value of 0.2 applied in equation 9 was chosen by an inspection of several scenes to limit the amount of false detection while maintaining the discrimination of sulphur dioxide plumes.

3. Detection Results

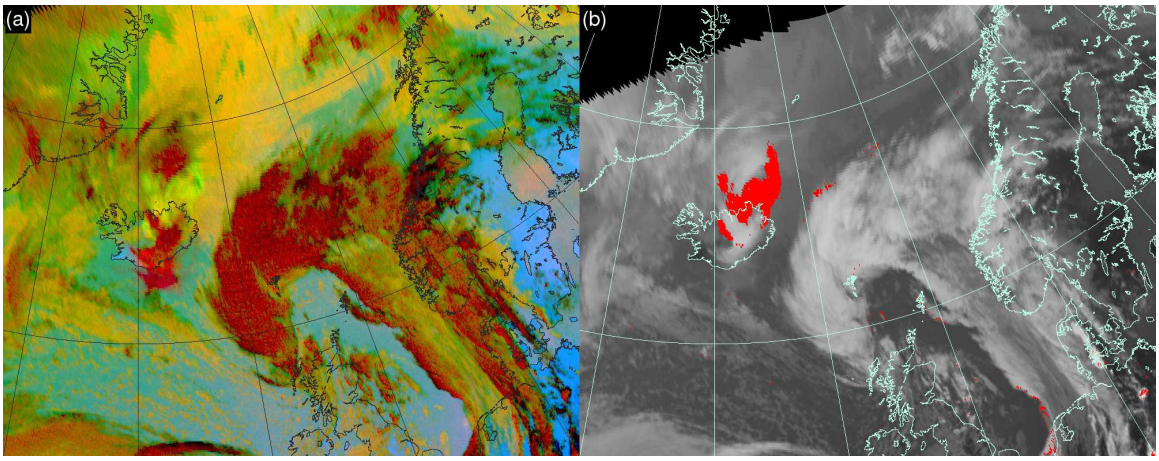

Figure 2: SEVIRI derived images from 22/05/2011 between 10:45 and 11:00 UTC. (a) Dust-RGB which shows the sulphur dioxide rich plume to the north of Iceland (green) with the ash rich plume to the south of Iceland (bright red) is partially covered by frontal cloud. (b) sulphur dioxide image derived using the "effective cloud emissivities" detection (detected sulphur dioxide in red).

Figure 2 shows the dust-RGB image and the improved sulphur dioxide product derived from SEVIRI data. The use of cloud emissivities has allowed the volcanic sulphur dioxide plume to be detected without the large number of false alarms shown for the brightness temperature method in figure 1. In particular the problems over the land

surfaces have largely been eradicated. However, there are still areas where false detection occurs, most notably at the edge of clouds and where there are localised convective clouds. Where the radiative signal of the cloud is small (such as at cloud edges) the variation in cloud emissivities with wavelength are hard to interpret and can lead to false detection. This could potentially be improved by identifying the pixels local radiative centre and using this to get a physically consistent discrimination (Pavolonis and Parker, 2010). Misalignment of pixels can also cause difficulties in detection at the cloud edges.

The detection of sulphur dioxide from hyperspectral sounders (such as AIRS and IASI) has been shown to be more sensitive than infrared imagers (such as MODIS and SEVIRI). The hyperspectral sounders have a detection ability comparable to the UV/visible sensors (OMI and GOME-2) which have a proven ability to detect sulphur dioxide to an accuracy of 1-2 DU (Krotkov et al., 2008). AIRS has 2000 channels and two channels can be selected which react similarly to water vapour and liquid water but have a significant difference in absorption by sulphur dioxide. Sulphur dioxide values derived from AIRS measurements using the technique of Prata and Bernardo (2007) are used to evaluate the region detected using MODIS data and the “effective cloud emissivities” approach described in section 2.

Figure 3 shows a side-by-side comparison of AIRS and MODIS sulphur dioxide detection for three volcanic plumes. MODIS and AIRS data were received as level 1 radiances and processed into sulphur dioxide plots at the Met Office. MODIS and AIRS are both on the Aqua satellite and will therefore be seeing the plumes at the same times and viewing angles. AIRS has a much larger footprint with approximately 190 MODIS pixels in the same area as one AIRS pixel (Schreier et al., 2010). The difference in resolution is evident in figure 3 with the plots derived from AIRS being blocky relative to the MODIS derived images.

The method suggested in this report and applied to MODIS data is capable of distinguishing pixels contaminated with high amounts of sulphur dioxide from other cloud affected and clear-sky data (figure 3). The area detected using MODIS covers a smaller area than the AIRS method because of higher spatial resolution and the technique is less sensitive. The AIRS sensitivity is thought to be 6 DU (Prata and Bernardo, 2007) while the infrared imagers are thought to have a lower sensitivity (~10 DU, Prata and Kerkmann, 2007). This will be investigated further in the following sections.

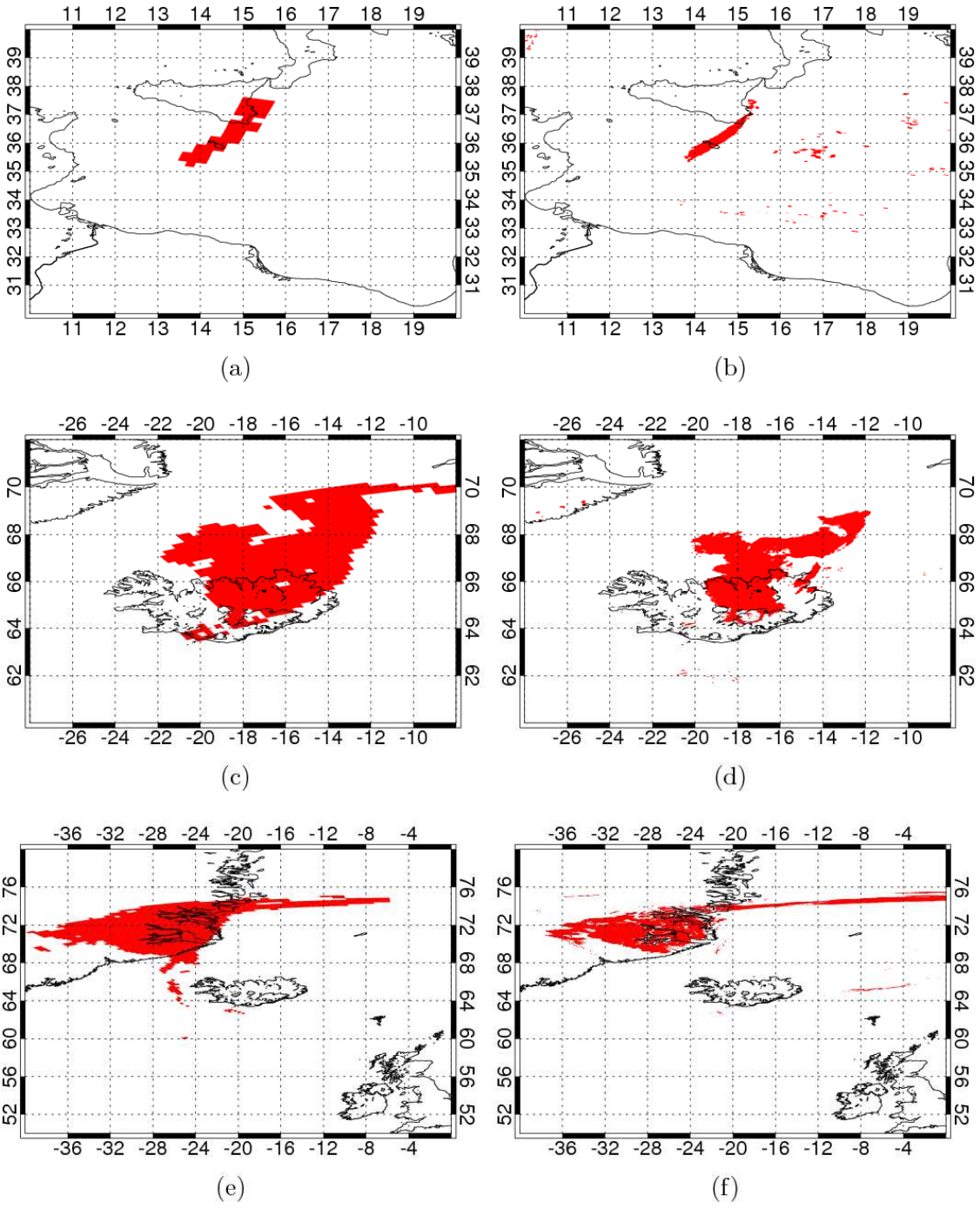

Figure 3: Comparison of the sulphur dioxide detection from AIRS using the methodology of Prata and Bernardo (2007) and MODIS using the "effective cloud emissivities" approach described in section 2, red areas are identified as anomalously high levels of sulphur dioxide. (a) and (b) are AIRS and MODIS, respectively, from Etna 13/01/2011 between 01:00-01:30 UTC. (c) and (d) are AIRS and MODIS, respectively, from Grimsvotn 22/05/2011 between 13:00-13:30 UTC. (e) and (f) are AIRS and MODIS, respectively, from Grimsvotn 23/05/2011 at 13:30-14:00 UTC.

4. Quantitative estimate of column loading

The best method for estimating the sulphur dioxide column loading would be to undertake a 1D-VAR retrieval with the column amount and plume height as the state variables. However RTTOV currently has sulphur dioxide in the mixed gases group rather than a separate species. This limits our ability to undertake a retrieval. Therefore we will use the information at 8.5-8.7 µm to get an estimate for the sulphur dioxide column loading.

Corradini et al, (2009) showed that the 8.5 µm window channel does not become saturated over the range of sulphur dioxide column loadings expected from a volcanic eruption (up to 200 DU). The 7.3 µm channels begins to become saturated above 100 DU because of the stronger absorption of sulphur dioxide in this region. The 8.5 µm channel is a window channel and so should be able to observe sulphur dioxide emissions down to the surface when no water or ice cloud is present. It should be noted that the sensitivity becomes very small when the plume is near the surface and the temperature of the air approaches the temperature of the surface. The column loading of sulphur dioxide can be evaluated using equations 10 and 11, viz.

$$\varepsilon(\lambda) = 1 - \exp\left(-\frac{k(\lambda) * L}{\cos\theta}\right) \qquad \textbf{Eq. 10}$$

$$L = -\frac{\cos\theta}{k(\lambda)} \ln(1 - \varepsilon(\lambda)) \qquad \textbf{Eq. 11}$$

where $\varepsilon(\lambda)$ is the emissivity of the sulphur dioxide plume at a given wavelength (λ), θ is the sensor zenith angle, $k(\lambda)$ is the sulphur dioxide absorption coefficient for a given wavelength (in (mill-atm-cm)$^{-1}$) and L is the mass loading (in mill-atm-cm). 1 DU of sulphur dioxide is equivalent to 1 milli-atm-cm. The 8.5 µm channel is used to calculate the mass loadings. The cos(θ) term corrects the data from a slant to a vertical column loading.

A layer height of 10 km is assumed which effects the cloud temperature used in calculating the layer emissivity using equations 4 and 5. If the actual temperature of the cloud is a lot smaller or larger than the temperature at 10 km this will produce an incorrect sulphur dioxide column loading estimate. For mid-latitude layers the tropopause will be close to 10 km therefore a large altitude difference will result in a warmer plume layer and thus a greater column loading. Therefore the assumption of 10

km will tend to bias the sulphur dioxide loading estimate low. The choice of 10 km allows us the state that the value calculated is a lower limit.

The technique employed for AIRS data (Prata and Bernardo (2007)) also assumes the plume is at a fixed height of 10 km. The absorption spectrum of sulphur dioxide around the strong absorption band at 7.3 μm (range used is between 7.14 μm and 7.69 μm) is used to evaluate a best-fit between the column loading and the spectral signature observed in a given pixel. In order to evaluate a suitable absorption coefficient ($k(\lambda)$) for a given imager channel (MODIS and SEVIRI) the AIRS sulphur dioxide column loading data is treated as "reference". The MODIS data are then scaled to the AIRS sulphur dioxide loading to produce an estimated column loading. The treatment of AIRS as the "reference" is justified because hyperspectral sounders are more sensitive to sulphur dioxide plumes than the imaging radiometers.

A best fit analysis between the AIRS derived sulphur dioxide column loading and values derived from MODIS data is used to derive a suitable sulphur dioxide absorption coefficient for the 8.5 μm channel of MODIS viz.

$$-\cos\theta * \ln(1-\varepsilon(8.5\mu m)) = L(AIRS) * k(8.5\mu m) \qquad \textbf{Eq. 12}$$

where θ is the MODIS satellite zenith angle averaged over the area of an AIRS pixel, ε(8.5 μm) is the emissivity calculated from MODIS (using equation 4 and assuming a plume height of 10 km) averaged over the area of an AIRS pixel, L(AIRS) is the sulphur dioxide column loading (DU) evaluated from AIRS data and k(8.5 μm) is the sulphur dioxide absorption coefficient suitable for the MODIS channel centred at 8.5 μm.

The analysis was conducted using the three plumes shown in figure 3. To compare like with like the MODIS emissivities and satellite zenith angles were averaged over an area equivalent to the AIRS pixel size. Figure 4 shows the comparison with a line of best fit forced through the origin which produces a gradient of 0.0095. The coefficient of determination (R^2) derived from the analysis in figure 4 was 0.78. This shows a significant positive relationship between the data.

There is significant spread in the data shown in figure 4 which results from the mapping of MODIS pixels to the AIRS footprint and differences in the techniques applied to MODIS and AIRS measurements. Approximately 190 MODIS pixels can fit into a single

AIRS footprint. The best fit analysis shown in figure 4 contains data where all the MODIS pixels in an AIRS footprint were flagged as sulphur dioxide contaminated. This quality control was used to limit problems at cloud edges. There are still errors in the mapping because the shape of the MODIS pixels within a given AIRS footprint were not considered. The layer emissivities calculated from MODIS data are dependent on the atmospheric temperature profile, the surface temperature and the observed radiance at 8.5 µm. The AIRS method is dependent on the spectral correlation between AIRS channels and the sulphur dioxide absorption spectrum between 7.14 µm and 7.69 µm. The techniques are very different and will therefore react differently to variability in the atmospheric profile leading to the spread observed in figure 4.

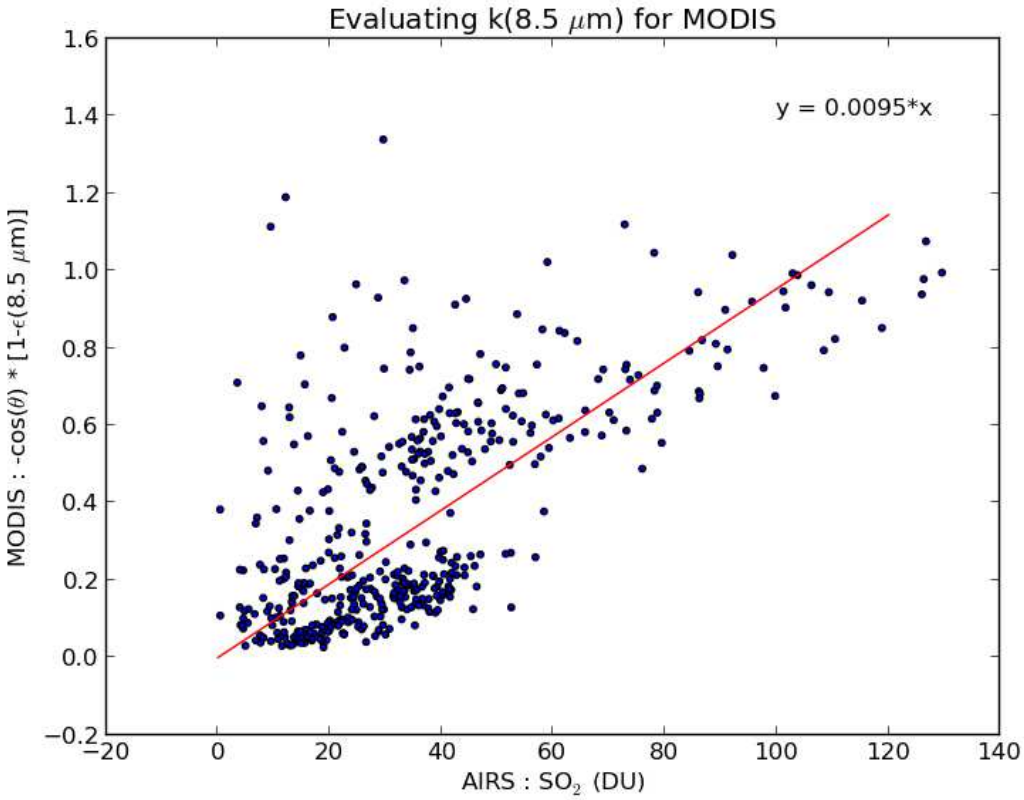

Figure 4: A plot of the MODIS derived sulphur dioxide emissivity at 8.5 µm averaged over the area of an AIRS pixel and the AIRS derived sulphur dioxide column loading. The line of best fit is shown in red and has been forced through the origin (the equation for the line of best fit is shown in the top right of the plot).

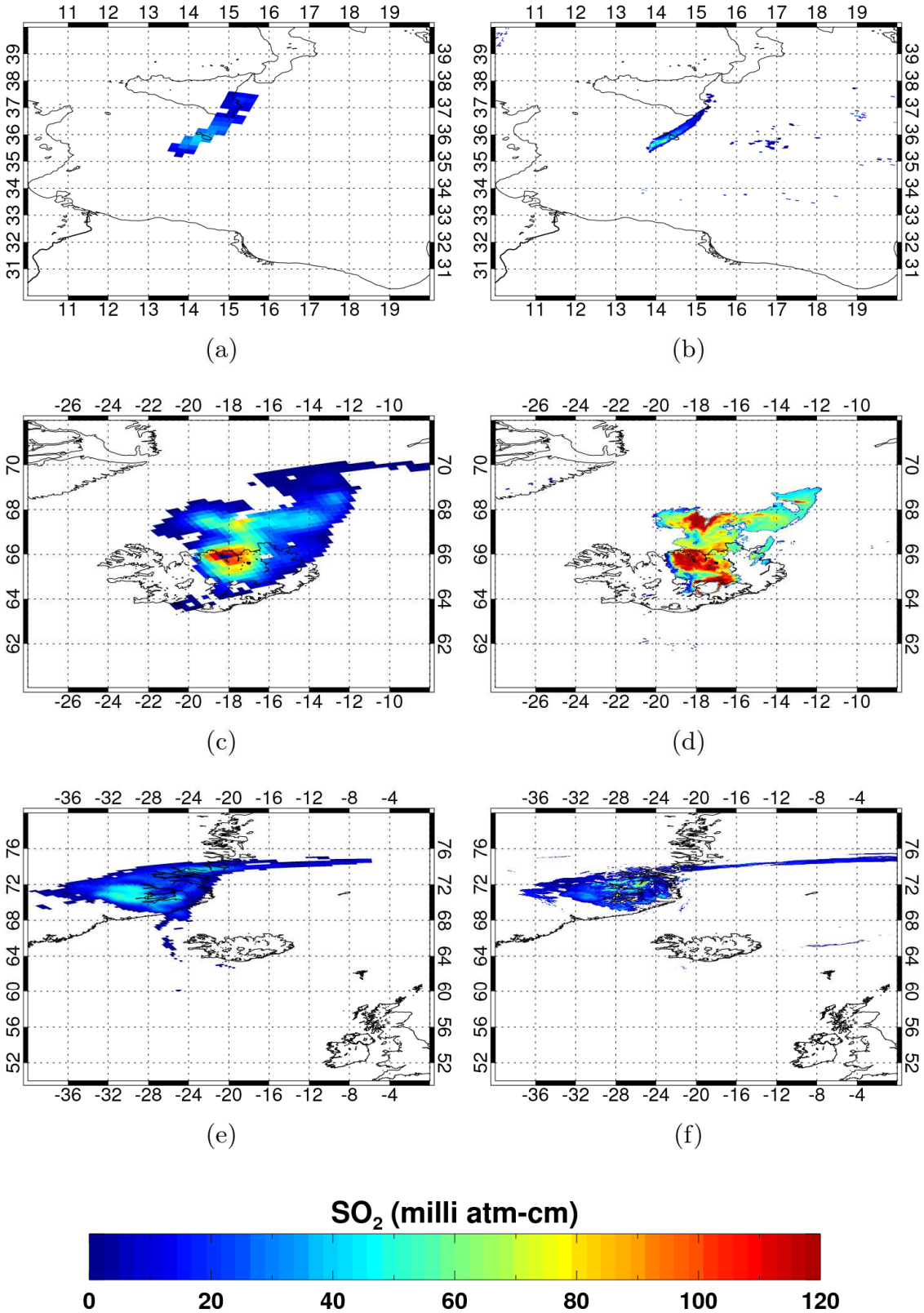

Figure 5: Comparison of the SO_2 mass loadings from AIRS using the methodology of Prata and Bernardo (2007) and MODIS using equation 11 and the scaling factor derived in figure 4. The subsections (a) to (f) are the same as in figure 3.

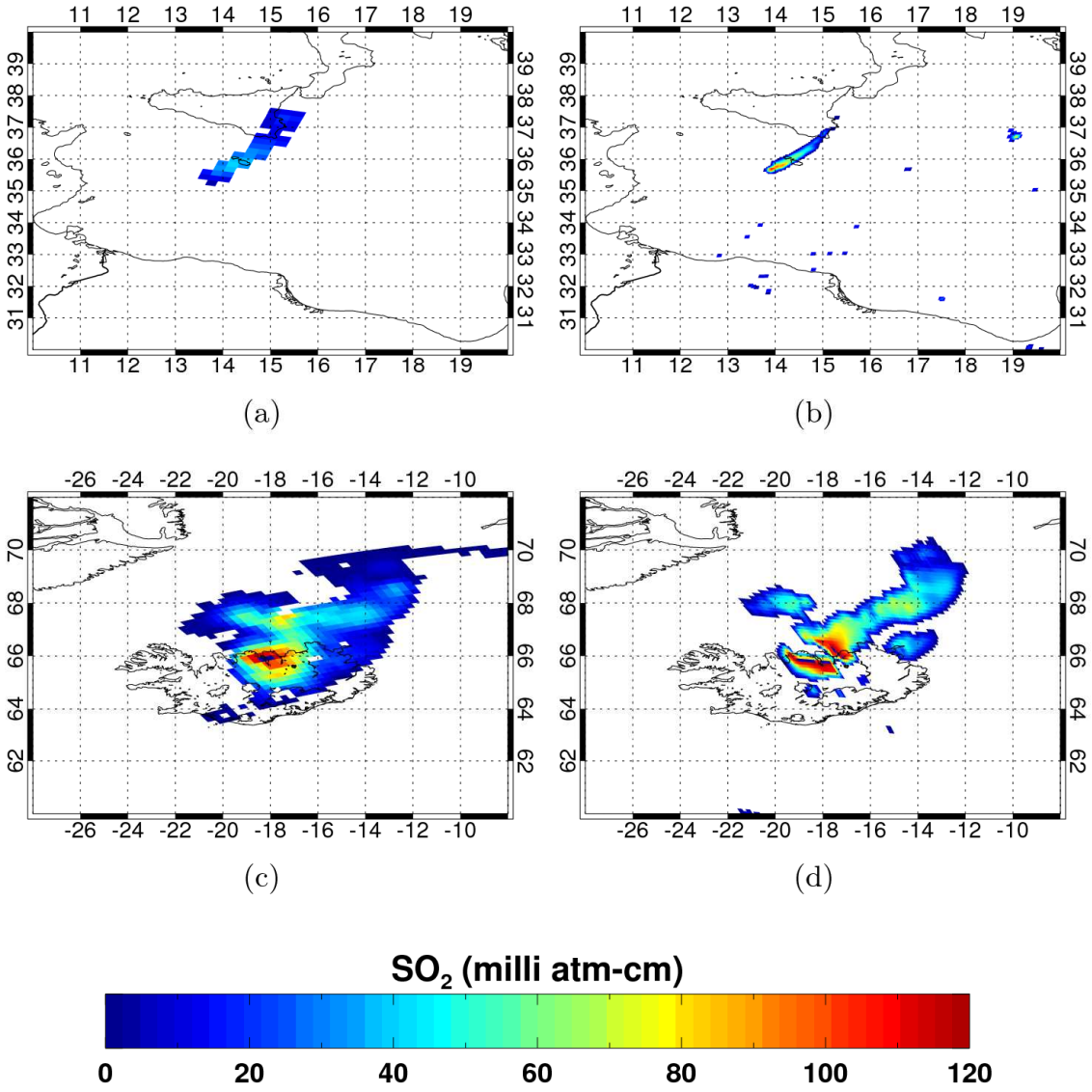

Figure 6: Images derived from SEVIRI data in comparison with AIRS sulphur dioxide column loadings. (a) and (b) are AIRS and SEVIRI, respectively, from Etna 13/01/2011 at 01:00-01:30 UTC. (c) and (d) are AIRS and SEVIRI, respectively, from Grimsvotn 22/05/2011 at 13:00-13:30 UTC.

The gradient of 0.0095 from the line of best fit in figure 4 is the k(8.5 µm) value that has been used to produce a column loading estimate from the MODIS data for the three cases in figure 3 and presented for visual comparison in figure 5. There is generally good visual agreement between the column loadings produced from the MODIS and AIRS data. The comparisons in figure 5 show that this technique applied to MODIS data is able to detect column loadings greater than approximately 10 DU. MODIS column loadings slightly over estimate the column loadings relative to AIRS for the plume on 22/05/2011 (figure 5(c) and 5(d)). There is a slight underestimation by MODIS for part of

the plume on 23/05/2011 (figure 5(e) and 5(f)). These differences are shown by the spread in figure 4. The evaluation of the absorption coefficient could be improved by including additional data and also by conducting detailed radiative transfer calculations.

Channel 7 on SEVIRI (centred at 8.7 µm) has a different spectral response function from band 29 on MODIS (band centred at 8.5 µm) and therefore a separate best fit analysis was conducted to calculate a sulphur dioxide absorption coefficient, k(8.7 µm), suitable for the 8.7 µm channel on SEVIRI. This best fit analysis uses equation 13 which is the same as equation 12 but for SEVIRI channel 8.7 µm viz.

$$-\cos\theta * \ln(1-\varepsilon(8.7\mu m)) = L(AIRS) * k(8.7\mu m) \qquad \textbf{Eq. 13}$$

For this analysis the plume shown in figure 3(e) was too far north for SEVIRI to capture therefore the best fit analysis was conducted with the two plumes shown in figure 3(a) and 3(c). The best fit analysis forced through the origin produced a gradient of 0.0046 with a coefficient of determination (R^2) of 0.81.

The value of 0.0046 derived from the best fit for SEVIRI is used to produce column loading estimates which are compared with AIRS data as shown in figure 6. The plume from the 23/05/2011 at 14:00 UTC has not been produced for the SEVIRI data because it is at too high latitude for SEVIRI which is onboard a geostationary platform. There is good visual agreement between the column loadings derived from SEVIRI and AIRS with both larger and smaller loadings captured. The limit of detection from SEVIRI appears to be around 10 DU similar to MODIS.

Figure 5 (b) and (d) can be compared directly with figure 6 (b) and (d), respectively. The comparisons show some differences in the detection and quantification between SEVIRI and MODIS. MODIS has a higher spatial resolution than SEVIRI and this is particularly evident to the north of Iceland (5(d) and 6(d)). However the differences between the column loadings derived from MODIS and SEVIRI are well within the region of uncertainty for the technique. The London VAAC would find the data from SEVIRI useful because of the high temporal resolution of the data (every 15 minutes). However the MODIS data provides a useful way of improving coverage north of Iceland and for comparison with the hyperspectral data to evaluate further the estimated column loadings produced.

5. Limitations of sulphur dioxide detection from infrared imagers

With infrared imagers there are only a limited number of channels. For example the SEVIRI instrument has 8 infrared channels compared with 2378 with a hyperspectral sounder such-as AIRS. In order to detect sulphur dioxide the strong absorption present in one of these channels is compared to other bands. However all of the infrared is affected by meteorological cloud and volcanic ash plumes with each of the 8 channels showing different signals dependent on the height and physical properties of the clouds. Also there is a water vapour absorption band and a carbon dioxide absorption band which further complicates the detection used with infrared imagers.

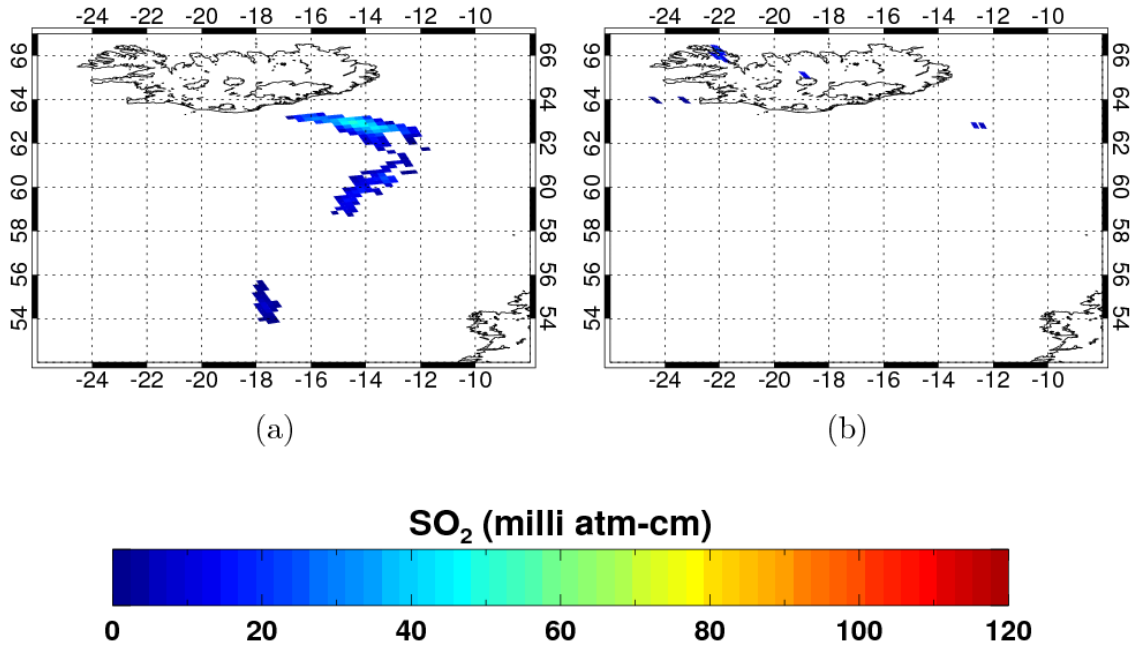

Figure 7: Sulphur dioxide column loading for the Eyjafjallajökull volcanic plume in 2010. (a) Prata and Bernardo (2007) technique applied to AIRS measurements made between 13:47 and 13:53 UTC on 06/05/2010. (b) Technique described in section 2 and 4 applied to SEVIRI measurements made between 13:45 and 14:00 UTC on 06/05/2010.

The use of an “effective cloud emissivities” approach as described in section 2 largely takes into account the effect of water vapour and carbon dioxide resulting in greater sensitivity to the layer properties relative to radiances alone. During a volcanic eruption volcanic ash is often co-located with sulphur dioxide. Sulphur dioxide is often used as a proxy for ash location (Carn et al., 2009). However, this co-location cannot always be relied upon because the ash and gas plumes can often be emitted at different times and heights.

Figure 7 shows an example where volcanic ash was co-located with sulphur dioxide and there is a significant effect on the radiance observed. The hyperspectral sounder, AIRS, is able to capture the anomalously high sulphur dioxide concentration (figure 7(a)) but these go undetected using the infrared imager detection technique described in section 2 (figure 7(b)). The AIRS technique uses the channels between 7.14 µm and 7.69 µm to detect and evaluate the sulphur dioxide loading, since there is little absorption by volcanic ash in this region. Volcanic ash absorbs more strongly at 12.0 µm and 13.4 µm than at 7.3 µm therefore the test described in equations 7 and 8 will be false and therefore the pixel will not be flagged as contaminated by sulphur dioxide for the infrared imagers.

The limited number of channels on an infrared imager result in the discrimination of sulphur dioxide only being possible when it is the dominant layer in a given pixel. Provided the effect of other clouds on the column is understood this technique can give useful information about the sulphur dioxide column loading and the presence of volcanic ash.

The quantitative estimate is dependent on the assumed temperature of the sulphur dioxide layer. If the sulphur dioxide plume is located at a height far from 10 km, which is assumed in the calculation, the plume temperature will be inaccurate and thus the quantitative estimate will be incorrect.

6. Conclusions

The detection method outlined in section 2 has shown the use of layer emissivities to improve the detection of high concentration sulphur dioxide plumes typical in certain volcanic eruptions. A method for estimating the column loading of sulphur dioxide from infrared imagers has been developed by comparison with a value derived from hyperspectral sounder (AIRS) measurements. Using small datasets the agreement with a line of best fit forced through the origin gives coefficients of determination (R^2) of 0.78 and 0.81 for MODIS and SEVIRI, respectively, showing significant positive correlations. Given the large footprint variation between AIRS and MODIS data this fit is sufficient to provide useful information to the London VAAC in the event of a volcanic eruption. The technique has also been applied to SEVIRI data with a separately derived sulphur dioxide absorption coefficient which also shows good visual agreement with column loadings derived from AIRS.

Future work should focus on performing calculations within RTTOV where sulphur dioxide is a variable gas to validate this scheme and potentially implement a 1D-var retrieval to improve the quantitative information. A 1D-var approach would improve understanding of how sulphur dioxide plumes affect each instrument channel and allow for the retrieval of plume height information.

Acknowledgments. Many thanks for comments and input from John Eyre, Roger Saunders, Sarah Millington and Peter Francis. I would like to acknowledge NASA for the MODIS data received via the Atmosphere Archive and Distribution System (LAADS), the Goddard Earth Sciences Data and Information Services Center for making the AIRS data available and EUMETSAT for the SEVIRI data which was obtained via EUMETCast.

Bibliography

Corradini, S., L. Merucci and A.J. Prata (2009) Retrieval of SO_2 from thermal infrared satellite measurements: correction procedures for the effects of volcanic ash, *Atmospheric Measurement Techniques*, 2, 177-191, doi:10.5194/amt-2-177-2009

Carn, S., A. Krueger, N. Krotkov, K. Yang and K. Evans (2009) Tracking volcanic sulphur dioxide clouds for aviation hazard mitigation, *Natural Hazards*, 51, 325–343, doi:10.1007/s11069-008-9228-4

Doutriaux-Boucher, M. and P. Dubuisson (2009) Detection of volcanic SO_2 by spaceborne infrared radiometers, *Atmospheric Research*, 92(1), 69-79, doi:10.1016/j.atmosres.2008.08.009

Halmer, M.M., H.U. Schmincke and H.F. Graf (2002) The annual volcanic gas input into the atmosphere, in particular into the stratosphere: a global data set for the past 100 years, *Journal of Volcanology and Geothermal Research*, 115 (3-4), 511-528, doi:10.1016/S0377-0273(01)00318-3

Hocking, J., P.J. Rayer, R.W. Saunders, M. Matricardi, A. Geer and P. Brunel (2011) RTTOV v10 Users Guide, http://research.metoffice.gov.uk/research/interproj/nwpsaf/rtm/docs_rttov10/users_guide_10_v1.3.pdf.

Krotkov, N.A., B. McClure, R.R. Dickerson, S. Carn, C. Li, P.K. Bhartia, K. Yang, A.J. Krueger, Z. Li, P.F. Levelt, H. Chen, P. Wang, and D. Lu (2008) Validation of SO_2 retrievals from the Ozone Monitoring Instrument over NE China, *J. Geophys. Res.*, 113, D16S40, doi:10.1029/2007JD008818.

Kuhn, P.M. (1963) Measured effective long-wave emissivity of clouds, *Mon. Wea. Rev.*, 91, 635-640.

Pavolonis, M.J. (2010) Advances in Extracting Cloud Composition Information from Spaceborne Infrared Radiances - A Robust Alternative to Brightness Temperatures. Part I: Theory, *Journal of Applied Meteorology and Climatology*, American Meteorological Society, 49, 1992-2012

Pavolonis, M.J. and A. Parker (2010) GOES-R Advanced Baseline Imager (ABI) Algorithm Theoretical Basis Document For SO_2 Detection, Version 1.0., draft report, NOAA, Silver Spring, Md.

Prata, A.J., W.I. Rose, S. Self and D.M. O'Brian (2003) Global, Long-Term Sulphur Dioxide Measurements From TOVS Data: A New Tool for Studying Explosive Volcanism and Climate, *Volcanism and the Earth's Atmosphere, Geophysical Monograph*, 139, 75–92, doi:10.1029/139GM05

Prata, A.J. and C. Bernardo (2007) Retrieval of volcanic SO_2 column abundance from Atmospheric Infrared Sounder data, *Journal of Geophysical Research*, 112, D20204, doi:10.1029/2006JD007955

Prata, A.J. and J. Kerkmann (2007) Simultaneous retrieval of volcanic ash and SO2 using MSG-SEVIRI measurements, Geophysical Research Letters, 34, L05813, doi: 10.1029/2006GL028691

Schreier, M.M., B.H. Kahn, A. Eldering, D.A. Elliot, E. Fishbein, F.W. Irion and T.S. Pagano (2010) Radiance Comparisons of MODIS and AIRS Using Spatial Response Information, Journal of Atmospheric and Oceanic Technology, 27, 1331-1342, doi:10.1175/2010JTECHA1424.1

Watson, I.M., V.J. Realmuto, W.I. Rose, A.J. Prata, G.J.S. Bluth, Y. Gu, C.E. Bader and T. Yu (2004) Thermal infrared remote sensing of volcanic emissions using the moderate resolution imaging spectroradiometer, *Journal of Volcanology and Geothermal Research*, 135 (1-2), 75-89, doi:0.1016/j.jvolgeores.2003.12.017